



HAL
open science

Human HOX Proteins Use Diverse and Context-Dependent Motifs to Interact with TALE Class Cofactors

Amélie Dard, Jonathan Reboulet, Yunlong Jia, Françoise Bleicher, Marilyne Duffraisse, Jean-Marc Vanaker, Christelle Forcet, Samir Merabet

► **To cite this version:**

Amélie Dard, Jonathan Reboulet, Yunlong Jia, Françoise Bleicher, Marilyne Duffraisse, et al.. Human HOX Proteins Use Diverse and Context-Dependent Motifs to Interact with TALE Class Cofactors. Cell Reports, 2018, 22, pp.3058 - 3071. 10.1016/j.celrep.2018.02.070 . hal-02996723

HAL Id: hal-02996723

<https://hal.science/hal-02996723>

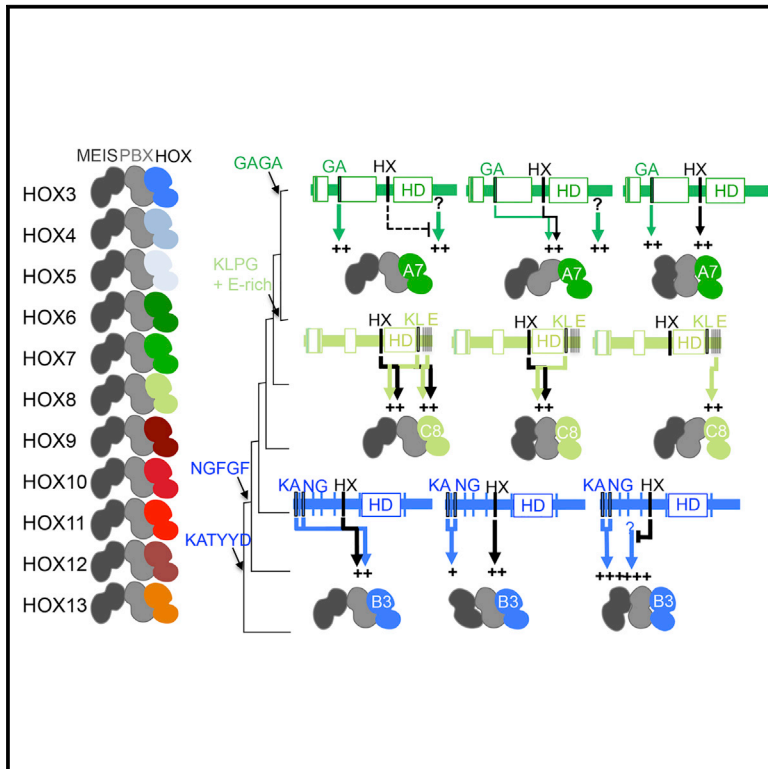
Submitted on 9 Nov 2020

HAL is a multi-disciplinary open access archive for the deposit and dissemination of scientific research documents, whether they are published or not. The documents may come from teaching and research institutions in France or abroad, or from public or private research centers.

L'archive ouverte pluridisciplinaire **HAL**, est destinée au dépôt et à la diffusion de documents scientifiques de niveau recherche, publiés ou non, émanant des établissements d'enseignement et de recherche français ou étrangers, des laboratoires publics ou privés.

Human HOX Proteins Use Diverse and Context-Dependent Motifs to Interact with TALE Class Cofactors

Graphical Abstract



Authors

Amélie Dard, Jonathan Reboulet, Yunlong Jia, ..., Jean-Marc Vanaker, Christelle Forcet, Samir Merabet

Correspondence

samir.merabet@ens-lyon.fr

In Brief

Dard et al. examine interaction flexibility between HOX proteins and TALE cofactors. The authors identify specific TALE-binding sites in different human HOX proteins. Most of these TALE-binding sites correspond to short motifs that are differently used depending on the DNA-binding site or cell context.

Highlights

- The vast majority of human HOX proteins use diverse TALE-binding sites
- The usage mode of TALE-binding sites is highly context specific
- Several identified TALE-binding sites are short linear interaction motifs
- A new TALE-binding site is important for the proliferative activity of HOXA7



Human HOX Proteins Use Diverse and Context-Dependent Motifs to Interact with TALE Class Cofactors

Amélie Dard,^{1,2} Jonathan Reboulet,^{1,2} Yunlong Jia,^{1,2} Françoise Bleicher,^{1,2} Marilyne Duffraisse,¹ Jean-Marc Vanaker,¹ Christelle Forcet,¹ and Samir Merabet^{1,3,*}

¹Institut de Génomique Fonctionnelle de Lyon, Université de Lyon, Université Lyon 1, CNRS, Ecole Normale Supérieure de Lyon, 46, allée d'Italie 69364 Lyon Cedex 07, France

²These authors contributed equally

³Lead Contact

*Correspondence: samir.merabet@ens-lyon.fr

<https://doi.org/10.1016/j.celrep.2018.02.070>

SUMMARY

HOX proteins achieve numerous functions by interacting with the TALE class PBX and MEIS cofactors. In contrast to this established partnership in development and disease, how HOX proteins could interact with PBX and MEIS remains unclear. Here, we present a systematic analysis of HOX/PBX/MEIS interaction properties, scanning all paralog groups with human and mouse HOX proteins *in vitro* and in live cells. We demonstrate that a previously characterized HOX protein motif known to be critical for HOX-PBX interactions becomes dispensable in the presence of MEIS in all except the two most anterior paralog groups. We further identify paralog-specific TALE-binding sites that are used in a highly context-dependent manner. One of these binding sites is involved in the proliferative activity of HOXA7 in breast cancer cells. Together these findings reveal an extraordinary level of interaction flexibility between HOX proteins and their major class of developmental cofactors.

INTRODUCTION

Hox genes code for homeodomain (HD)-containing transcription factors (TFs) that regulate numerous developmental processes during embryogenesis (Hueber and Lohmann, 2008). The diverse and specific transcriptional activities of Hox proteins often depend on the presence of two families of key cofactors that belong to the TALE (three amino acids loop extension) class of HD-containing TFs: PBC and MEINOX (Mukherjee and Bürglin, 2007). In vertebrates, the PBC family comprises Pbx1–4 proteins, while the MEINOX family includes Meis1–3 and Prep1 and 2 proteins (Longobardi et al., 2014). TALE cofactors are known to be important for several Hox developmental functions in vertebrates and invertebrates, regulating cell processes as diverse as apoptosis (Domsch et al., 2015), differentiation (Cerdá-Esteban and Spagnoli, 2014), or proliferation (Chen et al., 2016). Not surprisingly, these cofactors are also involved in

the oncogenic potential of HOX proteins in various solid cancers (Bhatlekar et al., 2014) and leukemia (Sitwala et al., 2008).

Given its major impact on development and disease, the partnership among HOX, PBX, and MEIS proteins has been the subject of numerous studies (Mann et al., 2009). Interaction between PBX and MEIS depends on evolutionarily conserved domains located in the N-terminal region of both proteins (Figure 1A). This interaction uncovers a nuclear localization signal in PBX, allowing its translocation into the nucleus *in vivo* (Berthelsen et al., 1999; Rieckhof et al., 1997). Original studies showed that mouse HOX proteins, with the exception of posterior paralog groups 11–13, can associate with PBX on DNA (Chang et al., 1995; Knoepfler and Kamps, 1995). HOX-PBX interactions involve a short HOX protein motif located upstream of the HD and called hexapeptide (HX) or W-containing motif (Figure 1A). This motif is present in all HOX members from paralog groups 1–10, and it is characterized by an invariant Trp residue located within a hydrophobic environment and followed by basic residues at +2 to +5 positions (In der Rieden et al., 2004). Crystal structures from *Drosophila* (Joshi et al., 2007; Passner et al., 1999) or mouse (LaRonde-LeBlanc and Wolberger, 2003; Piper et al., 1999) HOX/PBX complexes indicate a preponderant role of the Trp residue in establishing strong contacts within the hydrophobic pocket formed in part by the three extra residues of the HD of PBX. In contrast to these solid molecular analyses, the role of the HX as a key TALE interaction motif has only been demonstrated at the functional level in the case of the mouse HOXA1 protein (Remacle et al., 2004).

HOX proteins also form trimeric complexes with both PBX and MEIS cofactors (Shanmugam et al., 1999). These trimeric complexes are surprisingly much less studied although they represent an important fraction of HOX regulatory functions *in vivo* (Amin et al., 2015; Penkov et al., 2013). Recent work showed that five of the 39 murine HOX proteins (HOXB6, HOXB7, HOXB8, HOXA9, and HOXA10) could form trimeric complexes with PBX1 and MEIS1 in the absence of the HX motif (Hudry et al., 2012). The dispensability of the HX motif for complex formation with TALE cofactors was also observed in several *Drosophila* Hox proteins (Hudry et al., 2012). Moreover, the *Drosophila* Ultrabithorax (Ubx) and AbdominalA (AbdA) proteins were shown to accomplish Pbx-dependent functions without the HX motif and by using another short motif *in vivo* (Foos et al., 2015; Merabet et al., 2007, 2011).



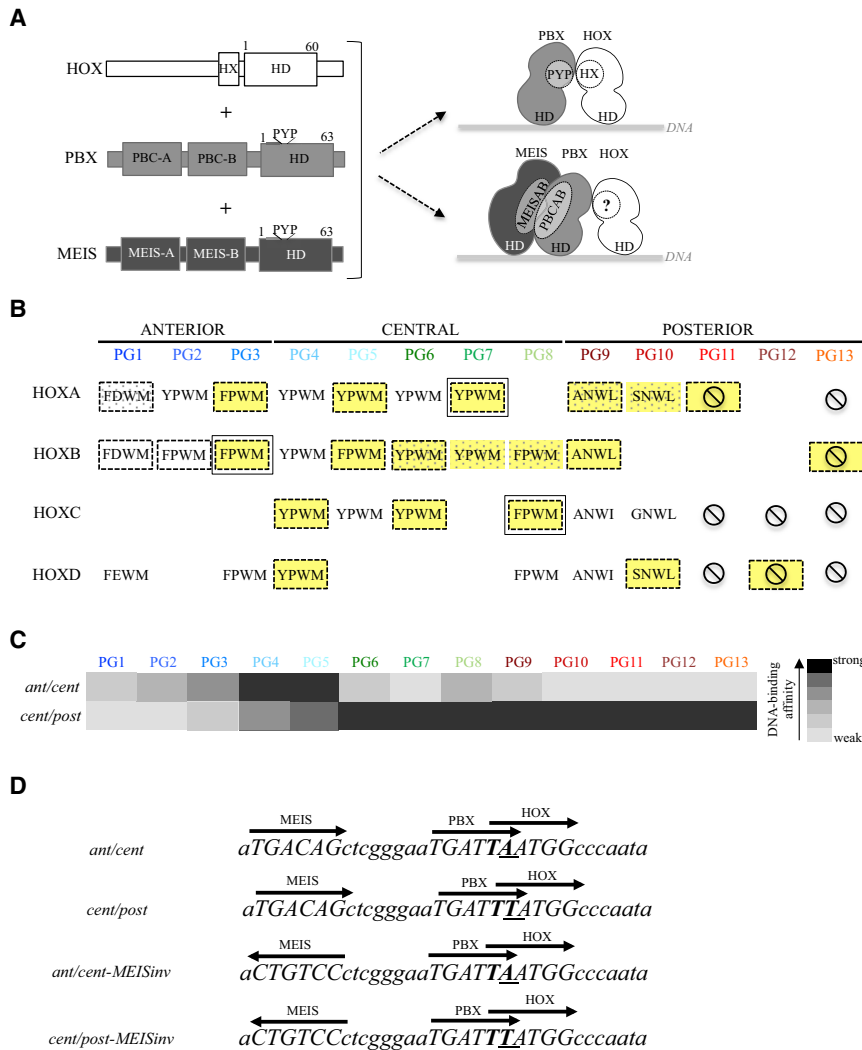


Figure 1. Assessing HOX-TALE Interaction Properties among All Mammalian HOX Paralog Groups

(A) Simplified representation of typical HOX, PBX, and MEIS proteins. The extra three PYP residues of the homeodomain (HD) of PBX participate in the formation of a hydrophobic pocket that makes strong interactions with the hexapeptide (HX) motif of HOX proteins in the context of dimeric HOX/PBX complexes. Molecular contacts are much less characterized in the context of a trimeric HOX-PBX-MEIS complex (indicated by the question mark).

(B) Sequence representation of the HX motif in each HOX paralog member in mammals. Note that the HX motif is limited to a unique conserved Trp residue in paralog groups 9 and 10 and that members of paralog groups (PG) 11–13 have no HX signature. Paralogs analyzed in this study are surrounded by a dotted line. Mouse HOX proteins that have previously been analyzed for their interaction properties with TALE cofactors are shaded (Hudry et al., 2012). Yellow background highlights HOX proteins displaying HX-independent interaction properties with PBX1 and MEIS1 (see also Figure 2). Solid black line indicates HOX proteins that are the subject of further molecular investigation in this study.

(C) DNA-binding affinity of HOX paralogs with PBX on two different consensus HOX/PBX-binding sites defined as anterior/central (ant/cent) or central/posterior (cent/post). This representation was adapted from *in vitro* studies with *Drosophila* Hox and TALE proteins (Slattery et al., 2011).

(D) Nucleotide sequence of probes used for electrophoretic mobility shift assays. Orientation and position of HOX-, PBX-, and MEIS-binding sites are indicated.

Altogether, these observations led to the proposition that molecular diversification in Hox-Pbx-Meis interaction properties could underlie paralog-specific functions of Hox proteins (Merafet and Mann, 2016). Although very appealing, this model awaits further experimental validation. In particular, the capacity to interact with TALE-class cofactors in the absence of the HX motif has not been demonstrated for Hox proteins of all paralog groups, and alternative TALE interaction motifs have not been described outside the *Drosophila* Ubx and AbdA proteins. Therefore, it remains to be established whether interactions between mammalian HOX proteins and the PBX and MEIS cofactors could rely on diverse and specific HOX protein signatures and whether this molecular complexity could constitute a general rule among all HOX paralog groups.

Here, we describe a systematic analysis of the interaction properties of 16 human and 3 mouse HOX proteins with the PBX1 and MEIS1 cofactors, taking into account all mammalian HOX paralog groups (Figures 1A and 1B). Our work relies on the molecular dissection of HOX-PBX1-MEIS1 interactions in different human cell lines and on various types of DNA-binding

sites *in vitro* (Figures 1C and 1D). Results show that HOX proteins from all except anterior paralog groups 1 and 2 are able to interact with PBX1 and MEIS1 in the absence of the HX motif. Analysis of complex formation with human HOX proteins from three different paralog groups further reveals the existence of specific TALE-binding sites that are evolutionarily conserved to different degrees. These TALE-binding sites are used with the HX motif in a DNA-binding site and cell-specific manner. One of these molecular signatures uncovers a motif that was functionally validated in the context of the proliferative activity of HOXA7 in breast cancer cells. This work definitively establishes the role of various and specific TALE-binding sites in human HOX proteins that helps us to understand HOX/TALE function during normal development and oncogenesis.

RESULTS

HOX Proteins from All but Paralog Groups 1 and 2 Interact with TALE Cofactors in the Absence of the HX Motif

The role of the HX motif was systematically analyzed by doing two complementary experimental approaches: bimolecular fluorescence complementation (BiFC) in live HEK293T cells, which

derive from human embryonic kidney, and electrophoretic mobility shift assays (EMSAs) *in vitro*. BiFC allows measuring global HOX-TALE interaction properties in the context of whole genomic DNA with its associated proteins. This method relies on the property of monomeric fluorescent proteins to be reconstituted from two separate sub-fragments upon spatial proximity (Kerppola, 2006). Importantly, BiFC was shown to be sensitive and specific enough to quantify subtle difference in protein-protein interaction affinities in different cell and animal contexts (Hudry et al., 2011, 2012). By comparison, EMSAs allow testing the role of the HX motif at the level of individual complexes on a single DNA-binding site. They were here realized on nucleotide probes containing a consensus binding site that is described to be preferentially recognized by anterior and central (ant/cent probe) or central and posterior (cent/post probe) HOX/PBX complexes (Figures 1C and 1D; Slattery et al., 2011). The two probes contain an additional MEIS-binding site with a consensus topology and sequence (Figure 1D; Hudry et al., 2012).

Practically, 19 HOX proteins fused to the N-terminal fragment of the Venus fluorescent protein (resulting in VN-HOX fusion proteins) were analyzed with PBX1 fused to the complementary C-terminal fragment of Venus (VC-PBX1). Since HEK293T cells express endogenous PBX1 and MEIS1 (Figures S1A–S1C), BiFC was performed without co-transfecting MEIS1. We anticipated that the nuclear localization of VC-PBX1 was, therefore, under the control of endogenous MEIS1, allowing the performance of BiFC to be with equal nuclear amounts of PBX1 and MEIS1 and in the context of a DNA-bound trimeric HOX/PBX1/MEIS1 complex. Specificity of BiFC was validated by the observation of a significant loss of fluorescent signals when expressing the VN-HOX or VC-PBX1 construct with the complementary VC or VN fragment or when using a mutation known to affect the ability of PBX1 to interact with HOX proteins (Figures S1D–S1F). BiFC was also systematically quantified by taking into account the efficiency of the transfection between the different conditions (Figures S1G and S1G'). Results showed that the HX mutation did not generally affect the interaction (Figures 2A and 2A'). More particularly, HX-mutated HOX proteins from paralog groups 3–10 did not display any significant loss of BiFC when compared to the respective wild-type HOX protein. A significant loss of BiFC signal was only observed in the case of HX-mutated HOX proteins from paralog groups 1 and 2 (with 50%–60% loss; Figures 2A and 2A'). In addition, BiFC revealed that HOXA11, HOXD12, and HOXB13, which are devoid of a consensus HX motif, could interact with PBX1 (Figures 2A and 2A').

Similarly, EMSAs showed that HX-mutated HOX proteins from all but paralog groups 1 and 2 could form a trimeric complex with PBX1 and MEIS1 (yellow dotted boxes in Figures 2B and 2B'). By contrast, the loss of the HX motif strongly affected dimeric complex formation in the case of all tested HOX proteins, except for HOXB6 (black dotted boxes in Figure 2B). These results indicate that the HX motif is a major PBX interaction motif in the context of HOX/PBX1 complexes but that it becomes largely dispensable in the context of HOX/PBX1/MEIS1 complexes. Thus, the role of MEIS1 in inducing HX-independent interaction properties could apply to the large majority of HOX paralog groups. Finally, both HOXA11 and HOXB13 could also interact with either PBX1 or PBX1 and MEIS1 (Figure 2B), confirming BiFC observations in

HEK cells. Previous study did not notice complex formation between those posterior HOX proteins and PBX1 on a different nucleotide probe (Phelan et al., 1995), highlighting that the DNA-binding site is not neutral on the HOX-TALE interaction mode (see also below).

To test the role of MEIS for revealing HX-independent interaction properties in HEK cells, we repeated BiFC in conditions where the endogenous level of MEIS was strongly decreased. This was accomplished by using double-stranded RNA (dsRNA) recognizing the MEIS1–3 isoforms (Figure S1H; Table S2), a condition that led to cytoplasmic localization of co-transfected VC-PBX1 (Figure S1I). BiFC was analyzed in the case of HOXB3 and HOXC8, which are the subject of further molecular dissections (see below). Results showed that BiFC with HX-mutated HOXB3 or HOXC8 was strongly affected (around 50% loss) in the presence of dsRNA against MEIS (Figures S1J–S1L'). Thus, decreasing the level of endogenous MEIS1 in HEK cells affects the ability of HOX proteins to interact with PBX1 without the HX motif. We hypothesize that a decreased level of endogenous MEIS1 could potentially lead to more dimeric HOX/PBX1 complexes in the nucleus (and conversely less trimeric HOX/PBX1/MEIS1 complexes), therefore revealing HX dependency for the interaction. As a corollary, this result also suggests that BiFC observed in normal condition in HEK cells corresponds to HOX-PBX1 interactions occurring for their large majority in the context of a trimeric complex with endogenous MEIS.

Taken together, EMSAs and BiFC confirm that the HX motif is largely dispensable among mammalian HOX paralogs when complex formation occurs with PBX1 and MEIS1 (highlighted by a yellow background in Figure 1B). The identity of TALE-binding sites that could be used in addition to or in place of the HX motif in HOX proteins remains, however, to be determined.

Because the only two characterized TALE-binding sites in HOX proteins (the HX and UbdA motifs) correspond to short linear interaction motifs (SLiMs), we made the assumption that human HOX proteins could also potentially use the same type of molecular features as alternative TALE-binding sites. SLiMs are usually not longer than 10 residues (Davey et al., 2012) and could be predicted by using the SLiMPred program (Mooney et al., 2012). This program can also predict the presence of ordered and disorganized regions. We applied SLiMPred on several human HOX proteins (data not shown), and we decided to dissect TALE interaction properties for three HOX proteins displaying distinct predicted intra-molecular organizations (human HOXB3, HOXA7, and HOXC8).

The Anterior HOXB3 Protein Contains Alternative TALE Interaction Motifs that Are Used in a Context-Dependent Manner

We first selected the anterior HOXB3 protein, which is predicted to contain at least ten conserved SLiMs and no long ordered regions (with the exception of the HD itself; Figure 3A). All but two SLiMs are located upstream of the HD. Given this global organization, we started the analysis with two deletions: a C-terminal deletion removing the two predicted motifs downstream of the HD and an N-terminal deletion removing five predicted SLiMs upstream of the HX motif (deletions dC and d100; Figure 3A). Deletions were analyzed in the context of wild-type or HX-mutated

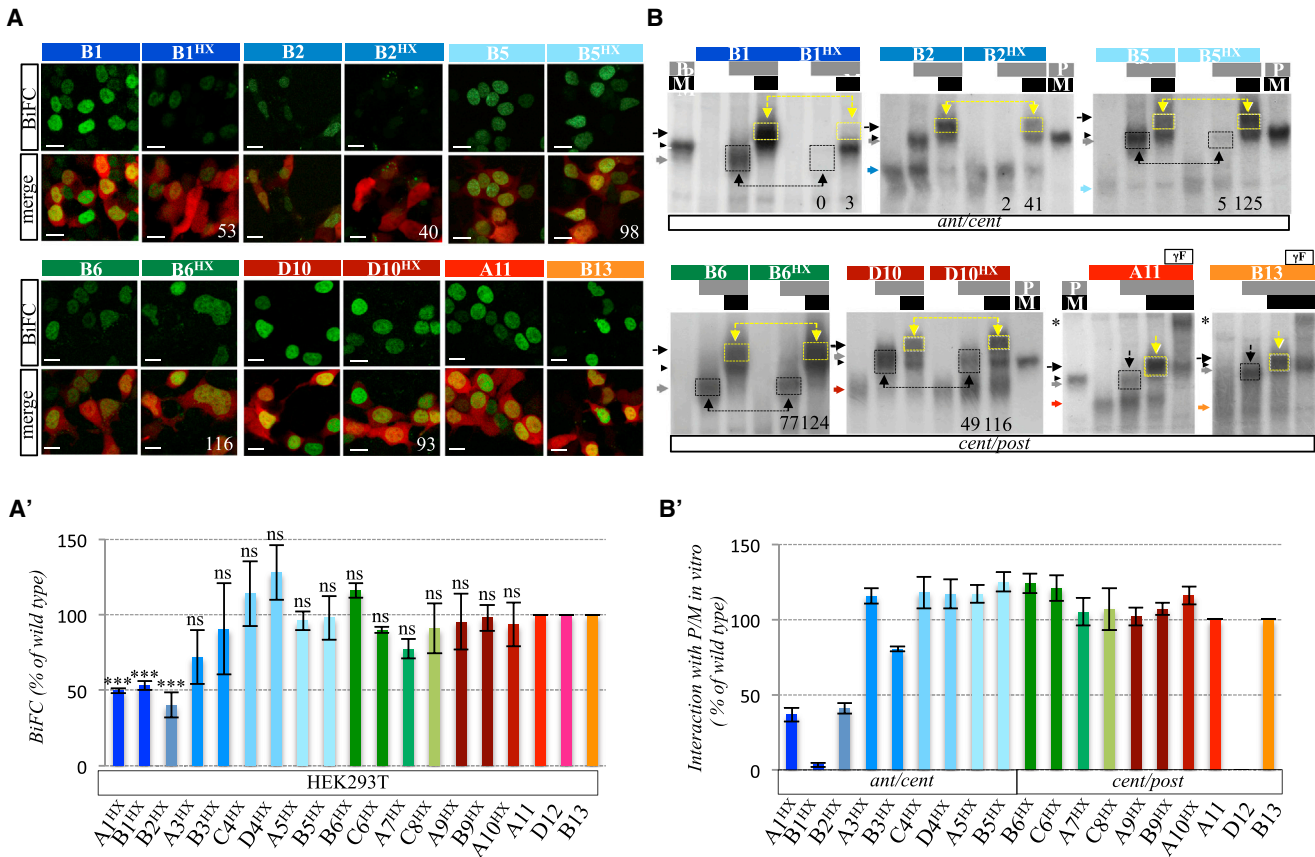


Figure 2. Interaction Properties among HOX, PBX1, and MEIS1 Proteins

(A) BiFC between wild-type or HX-mutated HOX proteins and PBX1 in live HEK293T cells, as indicated. An illustrative confocal picture is given for anterior, central, and posterior HOX representatives. Quantification of BiFC signals (green, upper pictures) with HX-mutated HOX proteins is provided as a percentage of the signal measured with the corresponding wild-type HOX protein. Quantification takes into account the efficiency of transfection, which is assessed by systematically co-transfecting a red fluorescent reporter. Scale bar, 10 μ m.

(A') Quantification of BiFC with HX-mutated HOX proteins. BiFC is strongly affected upon the HX mutation in the case of HOXA1, HOXB1, and HOXB2. The mean and SD are shown (from three independent experiments). Significance is shown relative to BiFC with the corresponding wild-type HOX protein and was evaluated by t test (** $p < 0.001$; ns, nonsignificant).

(B) Illustrative band shift experiments with wild-type or HX-mutated HOX proteins and PBX1 (P) and MEIS1 (M), as indicated. An illustrative gel is given for anterior, central, and posterior HOX representatives. Colored arrows indicate the monomer binding when present. Gray and black arrows depict dimeric and trimeric complexes with PBX1 or PBX1 and MEIS1, respectively. Black arrowhead indicates the PBX1/MEIS1 dimer. Gels have voluntarily been separated for each HOX protein to better illustrate the different complexes of different sizes. " γ F" indicates anti-FLAG antibody to supershift the FLAG-tagged HOX protein from the trimeric complex (star). The mean value of dimeric (black dotted boxes) or trimeric (yellow dotted boxes) complex formation with HX-mutated HOX proteins is given as a percentage of the complex obtained with the corresponding wild-type HOX protein.

(B') Quantification of trimeric complex formation with HX-mutated HOX proteins. The HX mutation does not affect complex formation in the presence of MEIS1 for all tested HOX proteins, except for HOXA1, HOXB1, and HOXB2. Bars represent mean \pm SD of three independent experiments.

HOXB3 to assess for a potential redundant function between different TALE interaction interface(s).

In vitro analysis on the consensus ant/cent DNA-binding site showed that the dC deletion did not change interaction properties of wild-type or HX-mutated HOXB3 with PBX1 and MEIS1 (Figure S2A'). By contrast, the d100 deletion significantly affected trimeric complex formation but only when the HX was also mutated (Figure S2A'). To identify alternative TALE-binding site(s) in the first 100 residues of HOXB3, we generated additional deletions that progressively removed the different predicted SLiMs (HOXB3d61, HOXB3d31, and HOXB3d21; Figure 3A). Results showed that removing the first 61 or 31 residues

of HOXB3 was sufficient to affect trimeric complex formation with PBX1 and MEIS1 in the context of the HX mutation (Figure S2A'). Interestingly, the short d21 deletion did not affect complex formation of HX-mutated HOXB3 (Figure S2A'). The region in between d21 and d31 deletions contains a predicted conserved SLiM with the core NGFGFD sequence (Figure 3A). We found that this motif was important for trimeric complex formation, but only when combined with the HX mutation and the d21 deletion (construct B3d21^{NG/HX}, Figure S2A'), suggesting that the first 21 residues of HOXB3 have also a redundant TALE interaction activity with the NGFGFD and HX motifs. This region contains two predicted SLiMs: one at the extreme N

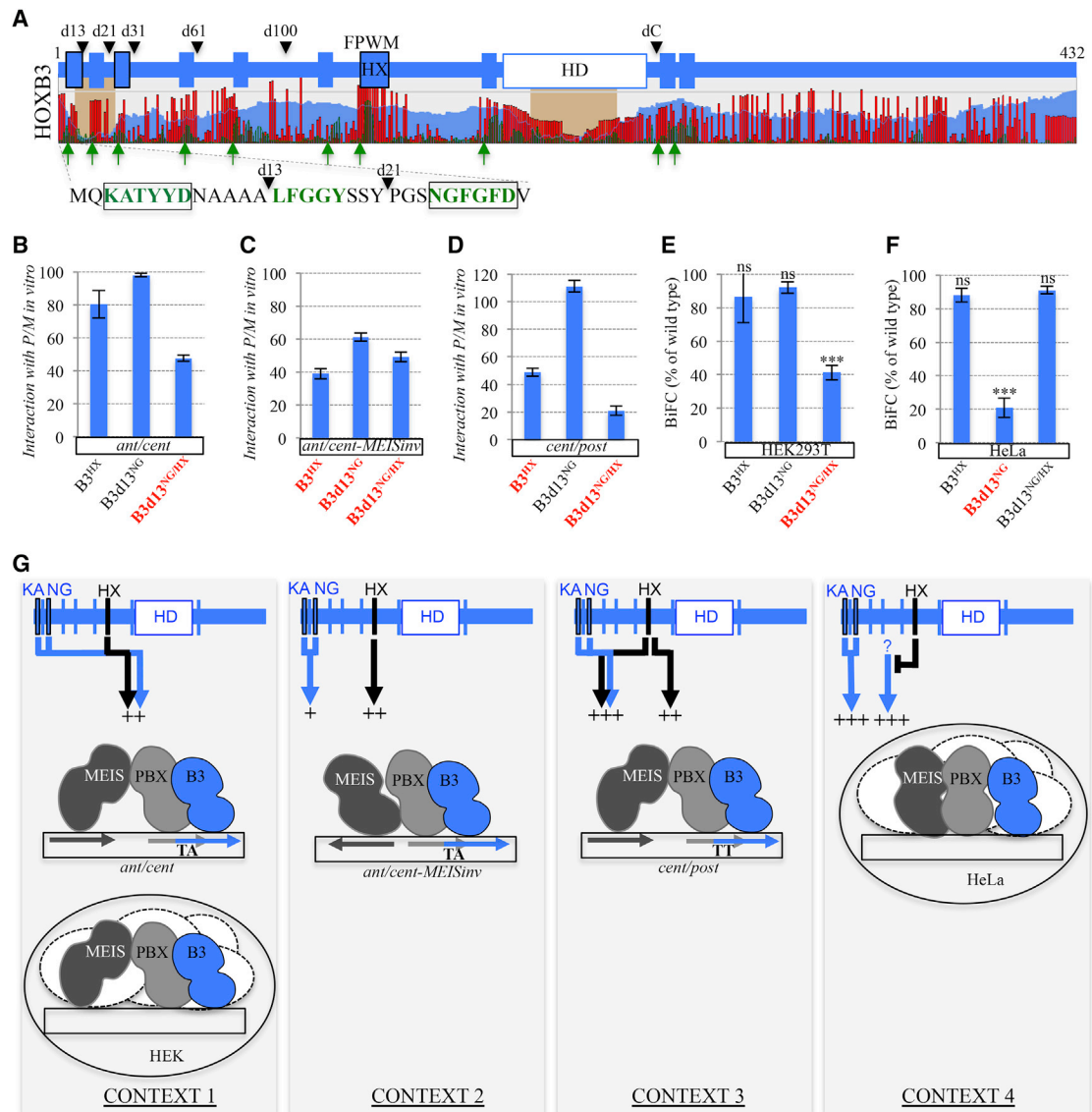


Figure 3. Deciphering Alternative TALE Interaction Properties in the Anterior Human HOXB3 Protein

(A) Global organization of HOXB3 with conserved predicted short linear motifs (SLIMs, green peaks and green arrows), ordered domains (brown blocks), and long disorganized regions (blue waves). Red peaks indicate the level of conservation of each residue among vertebrate species. A schematic representation of HOXB3 is shown above the picture, with deletions generated to identify TALE interaction regions. SLIMs are schematized by small boxes. Boxes surrounded by a black line depict SLIMs that are involved in the HOXB3-TALE interaction. The sequence of the N-terminal part of HOXB3 is indicated with the two alternative TALE interaction SLIMs (KATYYD and NGFGFD motifs, surrounded). Prediction was obtained by using SLiMPred0.9 (http://bioware.ucd.ie/~compass/biowareweb/Server_pages/slimpred_legacy.php).

(B–D) Quantifications of trimeric complex formation with mutated HOXB3 proteins on the *ant/cent* (B), *ant/cent-MEISinv* (C), or *cent/post* (D) nucleotide probe, as indicated. Bars represent mean \pm SD of three independent experiments. Mutations affecting the HOXB3-TALE interaction are highlighted in red.

(E and F) Quantification of BiFC with mutated HOXB3 proteins in HEK (E) or HeLa (F) cells, as indicated. Mutations affecting the interaction are highlighted in red. Significance is shown relative to BiFC with wild-type HOXB3 and was evaluated by t test (** $p < 0.001$; ns, nonsignificant). Bars represent mean of three independent experiments.

(G) Models recapitulating the context-specific use of the HX motif and alternative TALE interaction motifs in HOXB3. In context 1, the KATYYD, NGFGFD, and HX motifs have a redundant activity for HOXB3-TALE interaction, as observed on the *ant/cent* nucleotide probe *in vitro* and in live HEK cells. In context 2, the HX motif has a preponderant and independent role while the KATYYD and NGFGFD motifs act redundantly and have a minor contribution for HOXB3-TALE interaction, as observed on the *ant/cent-MEISinv* nucleotide probe *in vitro*. In context 3, the HX motif has a preponderant activity that is in part redundant with the KATYYD and NGFGFD motifs for HOXB3-TALE interaction, as observed on the *cent/post* nucleotide probe *in vitro*. In context 4, the KATYYD and NGFGFD motifs act redundantly and in addition to an unknown motif (indicated by the question mark) that is inhibited by the HX motif for HOXB3-TALE interaction, as observed in HeLa cells.

terminus, between residues 2 and 11, with a core KATYYDN sequence; and a second between residues 13 and 19, with a core LFGGY sequence (Figure 3A). Mutation of the LFGGY motif did not affect complex formation when combined to the NGFGFD and HX motif mutations (construct B3^{LF/NG/HX}; Figure S2A'). In contrast, removing the KATYYDN motif (by doing the d13 micro-deletion) affected complex formation when combined to the NGFGFD and HX motif mutations (construct B3d13^{NG/HX}; Figures 3B, S2A, and S2A'). Together these results reveal that HOXB3 contains three redundant TALE interaction motifs for complex formation with PBX1 and MEIS1 on the ant/cent nucleotide probe (corresponding to context 1 in Figure 3G).

Since the orientation of MEIS binding was shown to influence HOX-PBX-MEIS interaction properties (Hudry et al., 2012), we tested the role of the HX, KATYYDN, and NGFGFD motifs of HOXB3 in the context of the ant/cent probe containing an inverted MEIS-binding site (ant/cent-MEIS_{inv} probe; Figure 1D). In addition, we analyzed the role of the three TALE interaction motifs of HOXB3 on the cent/post nucleotide probe, therefore in the context of a less affine HOX/PBX-binding site. We observed that the activity of the three motifs was different in each case. On the ant/cent-MEIS_{inv} probe, the HX motif had a preponderant and non-redundant role with the KATYYDN and NGFGFD motifs for trimeric complex formation (Figures 3C and S2B, summarized in context 2 in Figure 3G). On the cent/post probe, the HX motif had a preponderant role that was in part redundant with the KATYYDN and NGFGFD motifs (Figures 3D and S2C, summarized in context 3 of Figure 3G). These results demonstrate that the DNA-binding site is not neutral for dictating the usage mode of TALE interaction motifs in HOXB3.

The various deleted and mutated forms of HOXB3 were also tested by doing BiFC with PBX1 in live HEK cells. These cells expressed a very weak level of endogenous HOXB3, and representative HOXB3 constructs were expressed at a similar range in the nucleus (Figures S2D–S2E'). BiFC analysis revealed a preponderant role of the region containing the KATYYDN and NGFGFD motifs in the context of the HX mutation (construct B3d31^{HX}; Figure S2F'). BiFC was also strongly affected upon the simultaneous loss of the KATYYDN, NGFGFD, and HX motifs, while the predicted LFGGY motif had no significant activity (Figures 3E, S2F, and S2F'). These results demonstrate a common redundant TALE interaction activity among the three motifs in HEK cells, as previously noticed on the ant/cent nucleotide probe *in vitro* (illustrated in the context 1 of Figure 3G).

Given the redundant TALE interaction activity among the KATYYDN, NGFGFD, and HX motifs on the ant/cent probe *in vitro* and in HEK cells, we asked whether the two alternative TALE interaction motifs of HOXB3 could also work in *trans* and be sufficient to rescue TALE interaction properties of an HX-deficient form of HOXA1. To this end, we generated chimeric proteins by fusing the N-terminal fragment of HOXB3 containing or not the KATYYDN and NGFGFD motifs to the HX-mutated part of HOXA1 (Figure S3A). Results showed that the presence of the N-terminal fragment of HOXB3 was sufficient to rescue the loss of complex formation of HX-mutated HOXA1 *in vitro* and in live HEK cells (Figures S3B–S3D'). Moreover, removing the KATYYDN and NGFGFD motifs in the HOXB3 fragment strongly impaired the interaction with TALE cofactors *in vitro* and in live cells (Figures

S3B–S3D'), demonstrating that the two motifs are important for the rescued activity of HX-mutated HOXA1.

Finally, the role of the HX, KATYYDN, and NGFGFD motifs was also analyzed in HeLa cells since their contribution was shown to be context dependent *in vitro*. BiFC showed a dispensability of the HX motif and a strict requirement of the KATYYDN and NGFGFD motifs in this additional cell context (Figures 3F and S2G). Moreover, the simultaneous loss of the three TALE-binding sites induced a rescue of the interaction (Figures 3F and S2G), suggesting that the HX motif could inhibit the activity of an additional and redundant TALE-binding site in the N-terminal part of HOXB3 (corresponding to context 4 in Figure 3G).

Altogether our analysis revealed the presence of at least three different TALE interaction motifs in HOXB3 that are used in a highly context-dependent manner.

The Central HOXA7 Protein Contains an Alternative TALE Interaction Motif that Is Used in a Context-Dependent Manner

The second HOX protein that we dissected was HOXA7, which was chosen based on its predicted intra-molecular organization that is broadly different from HOXB3. More particularly, HOXA7 contains only two conserved SLIMs in addition to the HX motif, and it has long ordered regions that encompass 70% of the protein sequence (including the HD; Figure 4A). Based on this prediction, we generated two N-terminal deletions that removed either one or the two predicted SLIMs (deletions d32 and d47; Figure 4A). As previously described for HOXB3, deletions were analyzed in the wild-type or HX mutant context.

In vitro analysis on the consensus cent/post probe revealed that the d32 deletion had no effect while the d47 deletion affected trimeric complex formation with a global loss of 55% (constructs A7dN32 and A7dN47; Figure S4A'). Surprisingly, the simultaneous mutation of the HX motif with the d47 deletion led to a partial rescue of trimeric complex formation while the dimeric complex remained strongly affected (construct A7dN47^{HX}; Figure S4A'). The motif located in between the d31 and d47 deletions corresponds to a core conserved GAGAGAF sequence (Figure 4A). To confirm that this motif could convey TALE interaction properties, we generated a small internal deletion removing specifically this sequence (construct A7dGA), and we analyzed the resulting effect in the context of full-length HOXA7, with or without the HX mutation. Results showed that this micro-deletion affected dimeric and trimeric complex formation in a range similar to the dN47 deletion *in vitro* (Figures 4B, S4A, and S4A'). Combining this micro-deletion with the HX mutation also led to a pronounced rescue of trimeric complex formation, suggesting that the two motifs have an antagonistic activity and that additional TALE interaction interface(s) could exist elsewhere in the protein (Figures 4B, S4A, and S4A', summarized in context 1 of Figure 4G). This hypothesis is also in accordance with the observation that the deletion of the GAGAF sequence did not lead to a complete loss of trimeric complex formation.

Since the DNA-binding site was shown to influence TALE interaction properties of HOXB3, we also analyzed the role of the HX and GAGA motifs on the cent/post nucleotide probe with an inverted MEIS-binding site and on the less affine ant/cent nucleotide probe. EMSAs showed that the single or

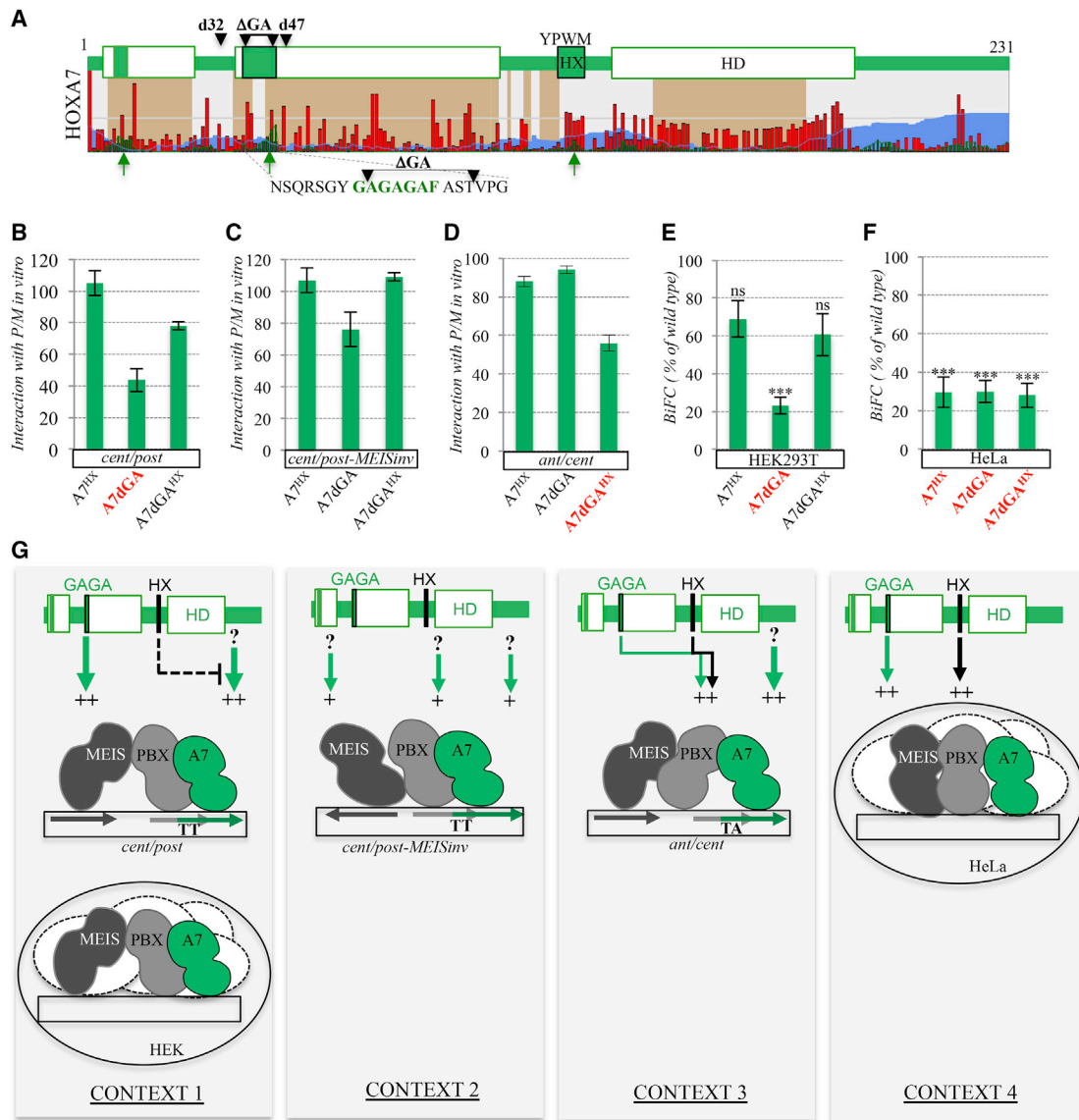


Figure 4. Deciphering Alternative TALE Interaction Properties in the Central Human HOXA7 Protein

(A) Global organization of HOXA7. Color code and symbols are as in Figure 3. The core sequence of the HX and GAGA motifs of HOXA7 is indicated. (B–D) Quantifications of trimeric complex formation with mutated HOXA7 proteins on the cent/post (B), cent/post-MEISinv (C), or ant/cent (D) nucleotide probe, as indicated. Bars represent mean \pm SD of three independent experiments. Mutations affecting the HOXA7-TALE interaction are highlighted in red. (E and F) Quantification of BiFC with mutated HOXA7 proteins in HEK (E) or HeLa (F) cells, as indicated. Mutations affecting the interaction are highlighted in red. Significance is shown relative to BiFC with wild-type HOXA7 and was evaluated by t test (***) $p < 0.001$; ns, nonsignificant). Bars represent mean of three independent experiments.

(G) Models recapitulating the context-specific use of the HX and GAGA motifs in HOXA7. In context 1, the GAGA motif has a preponderant role for HOXA7-TALE interaction, while the HX motif has an inhibitory role, potentially against another TALE-binding site that remains to be characterized (indicated by the question mark). This context was observed on the cent/post nucleotide probe *in vitro* and in HEK cells. In context 2, the HOXA7-TALE interaction relies on a TALE-binding site(s) other than the HX or GAGA motif (indicated by the question marks). This context was observed on the cent/post-MEISinv nucleotide probe *in vitro*. In context 3, the GAGA and HX motifs have a minor and redundant contribution for the HOXA7-TALE interaction, which suggests the role of other TALE-binding site(s) in HOXA7 (indicated by the question mark). This context was observed on the ant/cent nucleotide probe *in vitro*. In context 4, the GAGA and HX motifs have an independent and important contribution for the HOXA7-TALE interaction. This context was observed in HeLa cells.

combined loss of the HX and/or GAGA motif had no significant effect on the cent/post-MEISinv probe (Figures 4C and S4B), while the two motifs have a redundant activity on the ant/cent probe (Figures 4D and S4C). Together, these observations high-

light that the HX and GAGA motifs are used in a DNA-binding site-specific manner for complex assembly with PBX1 and MEIS1 (summarized in contexts 2 and 3 of Figure 4G, respectively).

Interaction properties were then analyzed at a larger scale level by doing BiFC in live HEK cells. These cells expressed very weak levels of endogenous *HOXA7*, and representative *HOXA7* constructs were expressed at a similar range in the nucleus (Figures S4D–S4E'). We observed that the d47 deletion or the micro-deletion of the GAGA motif had a strong effect on BiFC, with a global loss of 80% (Figures 4E, S4F, and S4F'). The simultaneous mutation of the HX motif also led to a significant rescue of complex formation, with BiFC levels comparable to levels obtained upon the single HX mutation (with 69% to 53% of remaining signals; Figures 4E, S4F, and S4F'). Thus, effects observed in HEK cells recapitulate effects observed *in vitro* on the consensus cent/post probe (context 1 in Figure 4G).

Finally, BiFC in HeLa cells showed that the HX and GAGA motifs have an independent contribution for *HOXA7*-TALE interaction (Figures 4F and S4G, summarized in context 4 of Figure 4G) and therefore distinct molecular properties when compared to HEK cells.

Altogether, *in vitro* and BiFC analyses showed the existence of a paralog-specific TALE-binding site in *HOXA7*. As previously noticed for *HOXB3*, the usage mode of TALE-binding sites in *HOXA7* is highly sensitive to the context, with redundant, opposite, or independent contributions, depending on the type of the DNA-binding site and cell environment.

The Central *HOXC8* Protein Contains Alternative TALE-Binding Sites that Are Used in a Context-Dependent Manner

The last HOX protein that we dissected was *HOXC8*, which has an intermediary intra-molecular organization when compared to *HOXB3* and *HOXA7*, with three conserved predicted SLiMs in addition to the HX and two small organized domains in addition to the HD (Figure 5A). Two predicted SLiMs are located in the N-terminal part of *HOXC8*. One of these motifs is conserved in other paralog groups and known to be important for the transcriptional activation potential of Hox proteins (the MSSYF motif; Tour et al., 2005). The third predicted SLiM is located immediately downstream of the HD and is followed by a repetition of Gln residues (Figure 5A). According to these predictions, we generated two different deletions removing either the N-terminal (deletion d109) or the C-terminal (deletion dC34) part of *HOXC8* (Figure 5A). Deletions were analyzed in the context of wild-type and HX-mutated *HOXC8*.

In vitro analyses on the consensus cent/post nucleotide probe showed that the N-terminal deletion had minor effects on trimeric complex assembly, even in the absence of the HX motif (Figure S5A'). By comparison, the C-terminal deletion led on its own to a global loss of 30% of trimeric complex formation, and the effect was dramatically enhanced in the context of the HX mutation, with only 23% of remaining trimeric complexes on average (construct *HOXC8*^{HX}dC34; Figure S5A'). Thus, the HX motif and C-terminal region have a redundant role for complex formation with TALE cofactors on the cent/post probe.

The C-terminal region of *HOXC8* contains a predicted conserved SLiM with a core KLPG sequence. To assess whether this motif could be involved in *HOXC8*-TALE interaction, we generated two additional constructs affecting either the KLPG

motif (mutation into Ala, construct *C8*^{KL}) or the Gln stretch (deleted construct *C8dE*). Analysis on the cent/post probe showed that the loss of either the KLPG motif or Gln stretch led to a loss of around 60% of trimeric complex when combined with the HX mutation (constructs *C8*^{HX/KL} and *C8*^{HX}dE; Figures 5B, S5A, and S5A'). This result shows that the KLPG motif and Gln stretch act redundantly with the HX motif and participate in two independent TALE interaction platforms for *HOXC8*-TALE complex formation on the consensus cent/post probe (corresponding to context 1 in Figure 5G).

HOXC8-TALE interaction properties were then dissected by doing BiFC in HEK cells. These cells expressed very weak levels of endogenous *HOXC8*, and representative *HOXC8* constructs were expressed at a similar range in the nucleus (Figures S5D–S5E'). N- and C-terminal deletions confirmed the preponderant role of the C-terminal part of *HOXC8* for the interaction with TALE cofactors, with around 50% loss of BiFC in the context of the HX mutation (Figures 5E and S5G). Surprisingly, removing the Gln stretch had no effect with or without the HX mutation, while the simultaneous mutation of the HX and KLPG motifs led to a global loss of 44% of BiFC (Figures 5E, S5F, and S5G). This result indicates that the HX and KLPG motifs act redundantly for complex formation with TALE cofactors in HEK cells (context 2 in Figure 5G). The fact that BiFC was not completely lost upon the HX and KLPG mutations also suggests that additional TALE-binding site(s) could exist in *HOXC8*.

Given the context-specific mode of activity for TALE-binding sites in *HOXB3* and *HOXA7*, we also analyzed TALE interaction properties of *HOXC8* on two additional nucleotide probes *in vitro* and in HeLa cells. We observed that the KLPG and HX motifs had a redundant activity, while the Gln-rich stretch was also independently required for trimeric complex formation on the cent/post-*MEISinv* (Figures 5C and S5B, summarized in context 3 of Figure 5G). The relationships between TALE-binding sites of *HOXC8* was different on the ant/cent probe, with a preponderant and unique role of the Gln-rich stretch (Figures 5D and S5C, summarized in context 4 of Figure 5G), and in HeLa cells, with a redundant activity of the HX motif and Gln repetition (Figures 5F and S5H, summarized in context 5 of Figure 5G). Together these results confirm that *HOXC8* is able to use various combinations of different TALE-binding sites depending on the DNA-binding site and cell context.

Finally, given that the KLPG motif could be redundant with the HX motif of *HOXC8* in several instances, we asked whether this alternative TALE interaction motif could also act *in trans* and rescue TALE interaction properties of HX-mutated *HOXA1*. To this end, we generated *HOXA1*-*HOXC8* chimeric proteins, with the same rationale as previously described for *HOXB3* and *HOXA7*. Here, the N-terminal fragment of *HOXA1*, mutated in the HX motif and containing the HD, was fused to the wild-type or KLPG-mutated C-terminal part of *HOXC8* (Figure S3E). Results showed that the C-terminal part of *HOXC8* could rescue the HX mutation of *HOXA1* *in vitro* and in HEK cells (Figures S3F–S3H'). Importantly, the KLPG mutation significantly affected the interaction (around 50% or 40% loss *in vitro* or in HEK cells, respectively; Figures S3G–S3H'), highlighting that

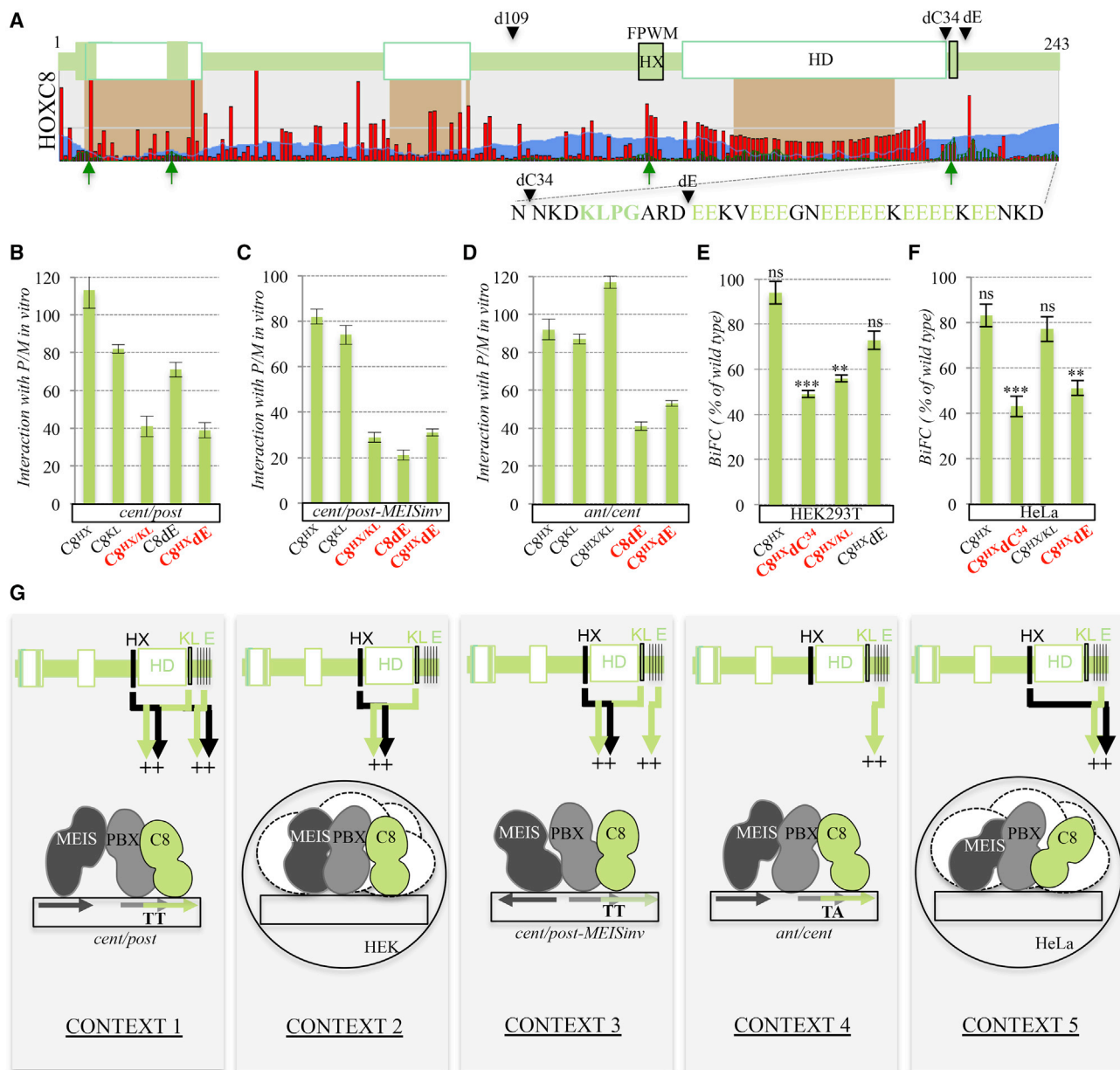


Figure 5. Deciphering Alternative TALE Interaction Properties in the Central Human HOXC8 Protein

(A) Global organization of HOXC8. Color code and symbols are as in Figure 3. The sequence of the C-terminal part with the KLPG motifs and stretch of Gln residues is indicated.

(B–D) Quantifications of trimeric complex formation with mutated HOXC8 proteins on the cent/post (B), cent/post-MEISinv (C), or ant/cent (D) nucleotide probe, as indicated. Bars represent mean \pm SD of three independent experiments. Mutations affecting the HOXC8-TALE interaction are highlighted in red.

(E and F) Quantification of BiFC with mutated HOXC8 proteins in HEK (E) or HeLa (F) cells, as indicated. Significance is shown relative to BiFC with wild-type HOXC8 and was evaluated by t test (** $p < 0.001$ and ** $p < 0.01$; ns, nonsignificant). Bars represent mean of three independent experiments. Mutations affecting BiFC are highlighted in red.

(G) Models recapitulating the context-specific use of the HX motif and alternative TALE-binding sites in HOXC8. In context 1, the HOXC8-TALE interaction relies on two independent interaction interfaces, one comprising the HX and KLPG motifs and the other the HX motif and Gln-rich region. This context was observed on the cent/post nucleotide probe *in vitro*. In context 2, the HOXC8-TALE interaction relies on the redundant activity of the HX and KLPG motifs. This context was observed in HEK cells. In context 3, the HOXC8-TALE interaction relies on two independent interaction interfaces, one comprising the HX and KLPG motifs and the other the Gln-rich region. This context was observed on the cent/post-MEISinv nucleotide probe *in vitro*. In context 4, the Gln-rich region has a preponderant role for the HOXC8-TALE interaction. This context was observed on the ant/cent nucleotide probe *in vitro*. In context 5, the HX motif and Gln-rich region act redundantly for the HOXC8-TALE interaction. This context was observed in HeLa cells.

the KLPG motif is important for the rescued activity of HX-mutated HOXA1.

The Paralog-Specific GAGA Motif of HOXA7 Is Important to Promote PBX-Dependent Proliferative Activities in Human Breast Cancer Cells

Since HOX members of the paralog group 7 have been shown to be involved in the progression and resistance to treatment of breast cancer cells (Jin et al., 2012), we tested whether the growth-promoting activity of HOXA7 on breast cancer-derived MCF7 cells could depend on the GAGA motif. MCF7 cells expressed endogenous *PBX1* but a very low level of *MEIS1* (Figure S1).

The role of the GAGA motif was first analyzed by doing BiFC in live MCF7 cells. Given the very low nuclear expression level of endogenous *MEIS1*, we performed bi-color BiFC by co-expressing CC-PBX1, CN-MEIS1, and VN-HOXA7 (Figure 6A) or Venus-based BiFC by expressing CC-PBX1 and VN-HOXA7 (Figure 6B). The same type of results was obtained in both cases, with no effect of the HX mutation while the GAGA mutation led to a strong decrease of fluorescence. Interestingly, the combined mutation of the HX and GAGA motifs led to a rescue of the HOXA7 interaction potential (Figures 6A', 6A'', 6B', and 6B''). Of note these different effects were not due to variations in the expression level of HOXA7 constructs (Figure 6C). Altogether these observations confirmed that the GAGA motif is important for HOXA7-PBX1 interaction in MCF7 cells.

We next investigated the role of the GAGA motif on HOXA7 proliferative activities. The experiment was realized without co-transfecting *PBX1* or *MEIS1* to measure HOXA7 proliferative activities in the presence of endogenous TALE cofactors. Transfection of wild-type HOXA7 led to a significant increase of cell proliferation, as previously described (Figure 6D; Zhang et al., 2013). The HX-mutated form of HOXA7 was even a more potent inducer of cell proliferation, suggesting that the HX motif could inhibit HOXA7 proliferative activities in this particular context (Figure 6D). Importantly, transfection of the GAGA-mutated HOXA7 protein did not increase the number of MCF7 cells when compared to the empty vector, highlighting that this motif is important for HOXA7 proliferative activities (Figure 6D). Interestingly, the combined HX and GAGA mutation led to a rescue of HOXA7 proliferative activities, thus recapitulating previous BiFC observations with *PBX1* (Figure 6D). Thus, the proliferative activity of HOXA7 in MCF7 cells seems to be controlled by a subtle balance between different interfaces that are able to promote or inhibit the interaction with *PBX1*.

DISCUSSION

Our work revealed the presence of highly diverse alternative TALE-binding sites that occupy various positions within the HOX protein. The usage mode of the different TALE-binding sites is also involving intra-molecular inhibitory loops, highlighting that the activity of the different TALE-binding sites is tightly controlled. This regulation *in cis* will differ depending on the cell environment and topology of DNA-binding sites. For

example, the inhibitory role of the HX motif in HOXA7 was observed in HEK and MCF7 cells, but not in HeLa cells.

We also noticed that alternative TALE-binding sites have a different degree of evolutionary conservation within the paralog group and among vertebrate lineages. This evolutionary plasticity does not only apply between different HOX proteins but also within the same HOX protein (Figure 7). For example, the KATYYD motif is more ancient and more widely conserved among vertebrate lineages than the NGFG(Y/F)(E/D) motif in members of the paralog group 3 (Figures 7A–7C).

Short protein motifs, or SLiMs, are by definition highly dynamic during evolution and are described to establish context-specific and low-affinity interactions (Davey et al., 2012). It is interesting to note that *Drosophila* Hox/TALE complexes were described to recognize low-affinity and divergent DNA-binding sites *in vivo* (Crocker et al., 2015). Alternative TALE interaction SLiMs could, therefore, be of great interest in this context, allowing HOX/TALE complexes to adapt their conformation on different types of DNA-binding sites. Such a molecular mode of action was noticed for the three dissected HOX proteins, which displayed a distinct requirement of their alternative TALE interaction motifs depending on the DNA-binding site and cell context. Altogether these observations underline that the choice of the TALE-binding site in the HOX protein is highly sensitive to the DNA and protein content environment.

In all tested HOX proteins, interaction properties with *PBX1* are strongly remodelled in the presence of *MEIS*. Future exciting challenges will be to decipher how the *MEIS* partner could induce such a strong molecular remodelling and how it could eventually impact on the HOX/TALE function *in vivo*. Interestingly, we observed that *PREP1* could not induce HX-independent interaction modes between *PBX1* and *HOXB3*, *HOXA7*, or *HOXC8* *in vitro* (Figure S6). Thus, the role of *MEIS* for diversifying HOX-PBX interaction modes appears very specific among the TALE family.

Cumulative data have established that HOX and TALE proteins could cooperate in several solid cancers (Bhatlekar et al., 2014) and leukemia (Sitwala et al., 2008). Disrupting this partnership could, therefore, constitute a promising strategy for therapeutic approaches. Accordingly, an HX-mimicking peptide has been described to induce apoptosis in several cancer cell lines, including breast cancer cells (Morgan et al., 2012). Interestingly, it was also noticed that MCF7 cells were relatively insensitive to the HX-mimicking peptide when compared to other breast cancer-derived cell lines (Morgan et al., 2012). Our work establishes that the majority of HOX proteins use additional TALE interaction interfaces that could act in a redundant, independent, or antagonistic way with the HX motif. In addition, the HX motif was recently shown to be important for promoting or inhibiting interactions with other types of cofactors (Baëza et al., 2015), suggesting that the effect of the HX-mimicking peptide could not be restricted to HOX-PBX interactions.

The identification of specific TALE interaction motifs could open new promising avenues for future therapeutic approaches against HOX/TALE-induced cancers. First, targeting these specific motifs is a way to inhibit the collaborative oncogenic activity of a specific HOX/TALE complex in cancer. We have identified

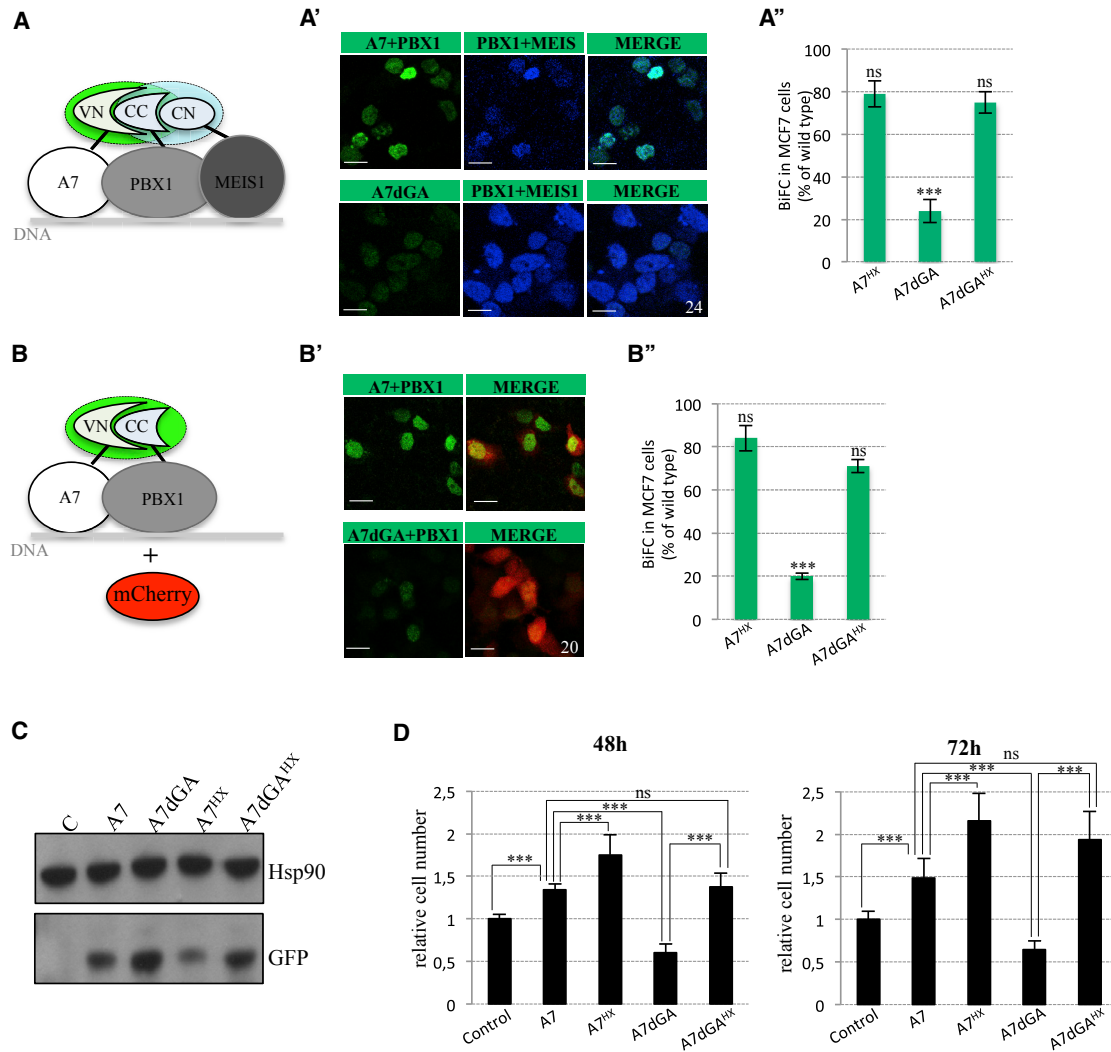


Figure 6. Role of the GAGA Motif on HOXA7 Proliferative Activities in MCF7 Cells

(A–A'') Bi-color BiFC in live MCF7 cells among the VN-HOXA7, CC-PBX1, and CN-MEIS1 constructs, as indicated. (A) Principle of the bi-color BiFC. (A') Illustrative confocal pictures of BiFC between HOXA7 constructs and PBX1 and MEIS1. (A'') Statistical quantification of BiFC. Loss of the GAGA motif affects BiFC. This effect is rescued by the HX mutation. Bars represent mean of three independent experiments. Significance is shown relative to BiFC with wild-type HOXA7 and was evaluated by t test (** $p < 0.001$; ns, nonsignificant).

(B–B'') Venus-based BiFC in live MCF7 cells between VN-HOXA7 constructs and CC-PBX1, as indicated. (B) Principle of the BiFC. (B') Illustrative confocal pictures of BiFC between HOXA7 constructs and PBX1. (B'') Statistical quantification of BiFC. The effect of the GAGA and/or HX mutation is as in A'. Bars represent mean of three independent experiments. Significance is shown relative to BiFC with wild-type HOXA7 and was evaluated by t test (** $p < 0.001$; ns, nonsignificant). Scale bar, 10 μ m.

(C) Western blot for the different VN-HOXA7 constructs used for the proliferative assay in MCF7 cells. Transfection efficiency was verified with the mCherry-expressing vector in each condition before preparing cell lysates. Cell lysates were subjected to immunoblot analysis with a GFP antibody (recognizing the VN fragment; see the [Experimental Procedures](#)) and HSP90 (as a loading control). A control (C) with only the mCherry-expressing vector is provided.

(D) Proliferative assay of MCF7 cells. The relative cell number is calculated 48 or 72 hr after transfection of the different constructs. Constructs are control (GFP-encoding plasmid), wild-type, HX-mutated, and/or GAGA-deleted HOXA7. The p value is reported by taking into account the transfection of wild-type HOXA7 as the reference condition. The relative cell number is significantly less important with the GAGA-deleted form of HOXA7. This effect is reversed by the HX mutation, reproducing BiFC observation with PBX1. Bars represent mean of three independent experiments in triplicate. Significance was evaluated by t test (** $p < 0.005$; ns, nonsignificant).

and confirmed the role of one such motif in HOXA7. Second, targeting these motifs has the potential to abolish the oncogenic activity in a specific cell context. This is an important parameter when considering that HOX proteins have a pro- or anti-oncogenic potential depending on the cell context considered ([Shah and Sukumar, 2010](#)).

EXPERIMENTAL PROCEDURES

For detailed methods, please see the [Supplemental Experimental Procedures](#).

BiFC Analysis in Live Cells

At 24 hr before transfection, 5×10^5 cells were plated on glass coverslips. Transfections were carried out using the JetPRIME reagent (Polyplus), with a

SUPPLEMENTAL INFORMATION

Supplemental Information includes Supplemental Experimental Procedures, six figures, and two tables and can be found with this article online at <https://doi.org/10.1016/j.celrep.2018.02.070>.

ACKNOWLEDGMENTS

We thank Robert K. Slany, Jacqueline Deschamps, and René Rezsöházy for reagents and Sylvie Di Ruscio for technical assistance. We thank René Rezsöházy and Yacine Graba for helpful comments on the manuscript. This work was supported by Association pour la Recherche sur le Cancer (ARC, PJA20141202007), Fondation pour la Recherche Médicale (FRM, DEQ20170336732), Ligue Nationale Contre le Cancer, Centre National de Recherche Scientifique (CNRS), CEFIPRA (5503-2), and Ecole Normale Supérieure (ENS) de Lyon.

AUTHOR CONTRIBUTIONS

Conceptualization, S.M.; Methodology, A.D., J.R., Y.J., F.B., and S.M.; Formal Analysis of Data, A.D., J.R., C.F., J.-M.V., and S.M.; Investigation, A.D., J.R., Y.J., F.B., M.D., C.F., and J.-M.V.; Writing – Original Draft, S.M.; Writing – Review & Editing, J.R., Y.J., F.B., C.F., and J.-M.V.; Funding Acquisition & Supervision, S.M.

DECLARATION OF INTERESTS

The authors declare no competing interests.

Received: August 27, 2017

Revised: January 12, 2018

Accepted: February 19, 2018

Published: March 13, 2018

REFERENCES

- Amin, S., Donaldson, I.J., Zannino, D.A., Hensman, J., Rattray, M., Losa, M., Spitz, F., Ladam, F., Sagerström, C., and Bobola, N. (2015). *Hoxa2* selectively enhances Meis binding to change a branchial arch ground state. *Dev. Cell* **32**, 265–277.
- Baëza, M., Viala, S., Heim, M., Dard, A., Hudry, B., Duffraisse, M., Rogulja-Ortmann, A., Brun, C., and Merabet, S. (2015). Inhibitory activities of short linear motifs underlie Hox interactome specificity in vivo. *eLife* **4**, 1–28.
- Berthelsen, J., Kilstrup-Nielsen, C., Blasi, F., Mavilio, F., and Zappavigna, V. (1999). The subcellular localization of PBX1 and EXD proteins depends on nuclear import and export signals and is modulated by association with PREP1 and HTH. *Genes Dev.* **13**, 946–953.
- Bhatlekar, S., Fields, J.Z., and Boman, B.M. (2014). HOX genes and their role in the development of human cancers. *J. Mol. Med. (Berl.)* **92**, 811–823.
- Cerdá-Esteban, N., and Spagnoli, F.M. (2014). Glimpse into Hox and tale regulation of cell differentiation and reprogramming. *Dev. Dyn.* **243**, 76–87.
- Chang, C.P., Shen, W.F., Rozenfeld, S., Lawrence, H.J., Largman, C., and Cleary, M.L. (1995). Pbx proteins display hexapeptide-dependent cooperative DNA binding with a subset of Hox proteins. *Genes Dev.* **9**, 663–674.
- Chen, J.Y., Miyayoshi, M., Wang, S.K., Yamazaki, S., Sinha, R., Kao, K.S., Seitla, J., Sahoo, D., Nakauchi, H., and Weissman, I.L. (2016). *Hoxb5* marks long-term haematopoietic stem cells and reveals a homogenous perivascular niche. *Nature* **530**, 223–227.
- Crocker, J., Abe, N., Rinaldi, L., McGregor, A.P., Frankel, N., Wang, S., Alsa-wadi, A., Valenti, P., Plaza, S., Payre, F., et al. (2015). Low affinity binding site clusters confer hox specificity and regulatory robustness. *Cell* **160**, 191–203.
- Davey, N.E., Van Roey, K., Weatheritt, R.J., Toedt, G., Uyar, B., Altenberg, B., Budd, A., Diella, F., Dinkel, H., and Gibson, T.J. (2012). Attributes of short linear motifs. *Mol. Biosyst.* **8**, 268–281.
- In der Rieden, P.M., Mainguy, G., Woltering, J.M., and Durston, A.J. (2004). Homeodomain to hexapeptide or PBC-interaction-domain distance: size apparently matters. *Trends Genet.* **20**, 76–79.
- Domsch, K., Papagiannouli, F., and Lohmann, I. (2015). The HOX-Apoptosis Regulatory Interplay in Development and Disease. *Curr. Top. Dev. Biol.* **114**, 121–158.
- Foos, N., Maurel-Zaffran, C., Maté, M.J., Vincentelli, R., Hainaut, M., Berenger, H., Pradel, J., Saurin, A.J., Ortiz-Lombardia, M., and Graba, Y. (2015). A flexible extension of the *Drosophila* ultrabithorax homeodomain defines a novel Hox/PBC interaction mode. *Structure* **23**, 270–279.
- Hudry, B., Viala, S., Graba, Y., and Merabet, S. (2011). Visualization of protein interactions in living *Drosophila* embryos by the bimolecular fluorescence complementation assay. *BMC Biol.* **9**, 5.
- Hudry, B., Remacle, S., Delfini, M.-C., Rezsöházy, R., Graba, Y., and Merabet, S. (2012). Hox proteins display a common and ancestral ability to diversify their interaction mode with the PBC class cofactors. *PLoS Biol.* **10**, e1001351.
- Hueber, S.D., and Lohmann, I. (2008). Shaping segments: Hox gene function in the genomic age. *BioEssays* **30**, 965–979.
- Jin, K., Kong, X., Shah, T., Penet, M.-F., Wildes, F., Sgroi, D.C., Ma, X.-J., Huang, Y., Kallioniemi, A., Landberg, G., et al. (2012). The HOXB7 protein renders breast cancer cells resistant to tamoxifen through activation of the EGFR pathway. *Proc. Natl. Acad. Sci. USA* **109**, 2736–2741.
- Joshi, R., Passner, J.M., Rohs, R., Jain, R., Sosinsky, A., Crickmore, M.A., Jacob, V., Aggarwal, A.K., Honig, B., and Mann, R.S. (2007). Functional specificity of a Hox protein mediated by the recognition of minor groove structure. *Cell* **131**, 530–543.
- Kerppola, T.K. (2006). Visualization of molecular interactions by fluorescence complementation. *Nat. Rev. Mol. Cell Biol.* **7**, 449–456.
- Knoepfler, P.S., and Kamps, M.P. (1995). The pentapeptide motif of Hox proteins is required for cooperative DNA binding with Pbx1, physically contacts Pbx1, and enhances DNA binding by Pbx1. *Mol. Cell. Biol.* **15**, 5811–5819.
- LaRonde-LeBlanc, N.A., and Wolberger, C. (2003). Structure of HoxA9 and Pbx1 bound to DNA: Hox hexapeptide and DNA recognition anterior to posterior. *Genes Dev.* **17**, 2060–2072.
- Longobardi, E., Penkov, D., Mateos, D., De Florian, G., Torres, M., and Blasi, F. (2014). Biochemistry of the tale transcription factors PREP, MEIS, and PBX in vertebrates. *Dev. Dyn.* **243**, 59–75.
- Mann, R.S., Lelli, K.M., and Joshi, R. (2009). Hox specificity unique roles for cofactors and collaborators. *Curr. Top. Dev. Biol.* **88**, 63–101.
- Merabet, S., and Mann, R.S. (2016). To Be Specific or Not: The Critical Relationship Between Hox And TALE Proteins. *Trends Genet.* **32**, 334–347.
- Merabet, S., Saadaoui, M., Sambrani, N., Hudry, B., Pradel, J., Affolter, M., and Graba, Y. (2007). A unique Extradenticle recruitment mode in the *Drosophila* Hox protein Ultrabithorax. *Proc. Natl. Acad. Sci. USA* **104**, 16946–16951.
- Merabet, S., Litim-Mecheri, I., Karlsson, D., Dixit, R., Saadaoui, M., Monier, B., Brun, C., Thor, S., Vijayraghavan, K., Perrin, L., et al. (2011). Insights into Hox protein function from a large scale combinatorial analysis of protein domains. *PLoS Genet.* **7**, e1002302.
- Mooney, C., Pollastri, G., Shields, D.C., and Haslam, N.J. (2012). Prediction of short linear protein binding regions. *J. Mol. Biol.* **415**, 193–204.
- Morgan, R., Boxall, A., Harrington, K.J., Simpson, G.R., Gillett, C., Michael, A., and Pandha, H.S. (2012). Targeting the HOX/PBX dimer in breast cancer. *Breast Cancer Res. Treat.* **136**, 389–398.
- Mukherjee, K., and Bürglin, T.R. (2007). Comprehensive analysis of animal TALE homeobox genes: new conserved motifs and cases of accelerated evolution. *J. Mol. Evol.* **65**, 137–153.
- Passner, J.M., Ryoo, H.D., Shen, L., Mann, R.S., and Aggarwal, A.K. (1999). Structure of a DNA-bound Ultrabithorax-Extradenticle homeodomain complex. *Nature* **397**, 714–719.
- Penkov, D., Mateos San Martín, D., Fernandez-Díaz, L.C., Rosselló, C.A., Torroja, C., Sánchez-Cabo, F., Warnatz, H.J., Sultan, M., Yaspo, M.L., Gabrieli, A.,

- et al. (2013). Analysis of the DNA-binding profile and function of TALE homeo-proteins reveals their specialization and specific interactions with Hox genes/proteins. *Cell Rep.* **3**, 1321–1333.
- Phelan, M.L., Rambaldi, I., and Featherstone, M.S. (1995). Cooperative interactions between HOX and PBX proteins mediated by a conserved peptide motif. *Mol. Cell. Biol.* **15**, 3989–3997.
- Piper, D.E., Batchelor, A.H., Chang, C.P., Cleary, M.L., and Wolberger, C. (1999). Structure of a HoxB1-Pbx1 heterodimer bound to DNA: role of the hexapeptide and a fourth homeodomain helix in complex formation. *Cell* **96**, 587–597.
- Remacle, S., Abbas, L., De Backer, O., Pacico, N., Gavalas, A., Gofflot, F., Picard, J.J., and Rezsőhazy, R. (2004). Loss of function but no gain of function caused by amino acid substitutions in the hexapeptide of Hoxa1 in vivo. *Mol. Cell. Biol.* **24**, 8567–8575.
- Rieckhof, G.E., Casares, F., Ryoo, H.D., Abu-Shaar, M., and Mann, R.S. (1997). Nuclear translocation of extradenticle requires homothorax, which encodes an extradenticle-related homeodomain protein. *Cell* **91**, 171–183.
- Shah, N., and Sukumar, S. (2010). The Hox genes and their roles in oncogenesis. *Nat. Rev. Cancer* **10**, 361–371.
- Shanmugam, K., Green, N.C., Rambaldi, I., Saragovi, H.U., and Featherstone, M.S. (1999). PBX and MEIS as non-DNA-binding partners in trimeric complexes with HOX proteins. *Mol. Cell. Biol.* **19**, 7577–7588.
- Sitwala, K.V., Dandekar, M.N., and Hess, J.L. (2008). HOX proteins and leukemia. *Int. J. Clin. Exp. Pathol.* **1**, 461–474.
- Slattery, M., Riley, T., Liu, P., Abe, N., Gomez-Alcala, P., Dror, I., Zhou, T., Rohs, R., Honig, B., Bussemaker, H.J., and Mann, R.S. (2011). Cofactor binding evokes latent differences in DNA binding specificity between Hox proteins. *Cell* **147**, 1270–1282.
- Tour, E., Hittinger, C.T., and McGinnis, W. (2005). Evolutionarily conserved domains required for activation and repression functions of the Drosophila Hox protein Ultrabithorax. *Development* **132**, 5271–5281.
- Zhang, Y., Cheng, J.C., Huang, H.F., and Leung, P.C.K. (2013). Homeobox A7 stimulates breast cancer cell proliferation by up-regulating estrogen receptor-alpha. *Biochem. Biophys. Res. Commun.* **440**, 652–657.